2013 IREP Symposium-Bulk Power System Dynamics and Control –IX (IREP), August 25-30, 2013, Rethymnon, Greece

Study of Subsynchronous Resonance in Meshed Compensated AC/DC Network

Atia Adrees and J. V. Milanović
School of Electrical and Electronic Engineering, University of Manchester, UK
(email: atia.adrees@postgrad.manchester.ac.uk, milanovic@manchester.ac.uk)

Abstract

The paper investigates the risk of subsynchronous resonance (SSR) in meshed power networks with compensated AC lines operating in parallel to voltage source converter (VSC) HVDC lines. Different compensation levels of AC line, different power transfer through VSC HVDC line and various contingencies are considered to assess the risk of mechanical torques amplification in turbine shaft due to SSR. Both, active and passive compensation of AC lines are considered.

Introduction

Electric power transmission networks are undergoing continuous changes and restructuring to accommodate integration of renewable generation and facilitate efficient operation of electricity markets. Planning consent for new overhead lines is becoming increasingly difficult if not impossible to obtain in many cases. Moreover, building new transmission lines requires longer time and considerably higher costs compared to passive (or even active) series compensation of existing lines.

Series compensation of transmission line facilitates higher power transfer, contributes towards angular and voltage stability of the network by reducing transmission angle and enabling dynamic contribution of reactive power. Voltage source converter (VSC) based HVDC systems with higher power transfer capabilities per line, independent control of active and reactive power flow and no technical line length limitations are also an attractive alternative for an AC system. Therefore, future electricity transmission networks are expected to incorporate a large number of VSC HVDC lines resulting into many instances where VSC HVDC lines might be operating in parallel with existing uncompensated or compensated AC lines.

It is well known that the presence of fixed series compensation, in particular, and HVDC controller can give rise to subsynchronous resonance [1, 2]. Dynamic instability due to SSR results in sustained or continuously growing high amplitude mechanical torques in turbine generator shaft. Similarly, transient torque amplification yields high amplitude shaft torques following system electrical disturbances and leads to shaft fatigue. SSR phenomenon has been studied extensively with fixed series compensation and line commutated converter (LCC) HVDC systems in the past [3-5]. A few studies have also been performed with VSC HVDC system [6, 7]. Most of the past SSR studies, however, were limited to rather small AC system or single line DC system.

Generators in a meshed network are generally at lower risk of dynamic instability due to SSR. However, there will always be contingencies in which the generator ends up being connected radially to the compensated line/ HVDC line or both of them. Moreover, transient torque amplification depends on electrical components, fault clearing time, breaker operation and modal damping. Future transmission networks topology may also change considerably in order to increase the efficiency of their operation. All these factors necessitate SSR risk assessment in a meshed network to assure shaft integrity and system stability.

This paper presents SSR studies in a large power network featuring two VSC HVDC lines operating in parallel to compensated AC lines. Case studies include different system contingencies, different power transfer through HVDC lines and different compensation levels, both active (using TCSCs) and passive (fixed capacitors) compensation. The studies illustrate the effect of VSC HVDC lines in different contingencies, combination of compensation levels and power transfer through the HVDC lines on risk of SSR in the network.

Test Network

The test network within the studies is a modified version of New England Test System and New York Power system presented in Fig. 1. Full system details and

978-1-4799-0199-9/13/$31.00 ©2013 IEEE

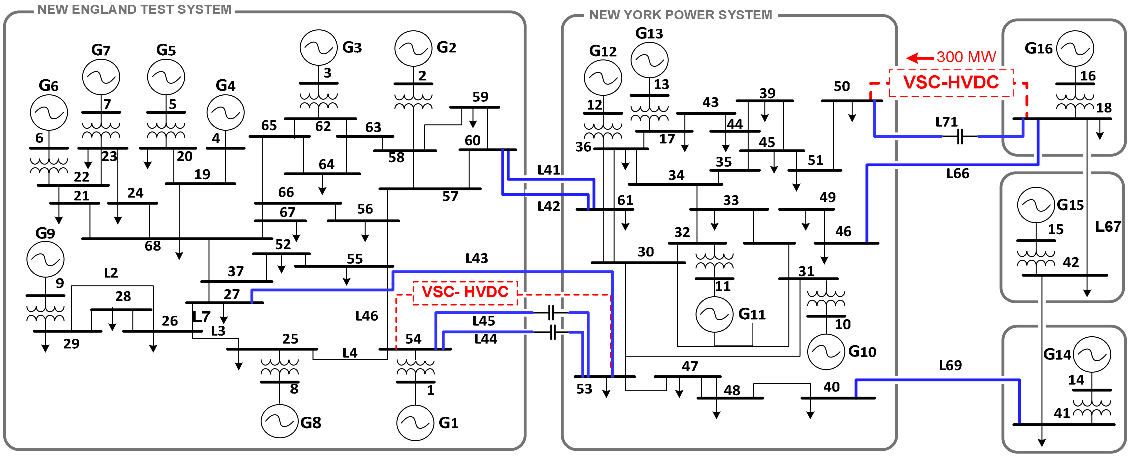

Fig. 1: 16 Machine, 68 bus network with two VSC HVDC links and three compensated lines

parameters can be found in [8]. This IEEE 16 machine, 68 bus network consists of five separate areas: NETS includes G1-G9; NYPS consists of generators G10-G13 and three further infeeds from neighboring areas are represented separately by equivalent generators G14, G15 and G16. With loading details in [8], NYPS area is importing power from the neighboring areas due to generation shortage of approximately 2.7GW. The power transfers through the inter-area ties are given below in Table I.

Table I: Active power imported into NYPS from surrounding areas

Active power imported from		To NYPS		Active Power (MW)
area	Bus#	Bus #	Line #	
NETS	60	61	L41 &L42	404.9
NETS	27	53	L43	27.6
NETS	54	53	L44 & L45	276.8
G14	41	40	L69	588.7
G16	18	46	L66	364.1
G16	18	50	L71	786

Two VSC HVDC lines are installed in parallel with two existing most heavily loaded AC lines, directly connected to clusters of generators in different areas of the network. Generator G16 is a dynamic equivalent of the area; therefore, it is replaced with a small network of equivalent inertia and active power shown in Fig. 2.

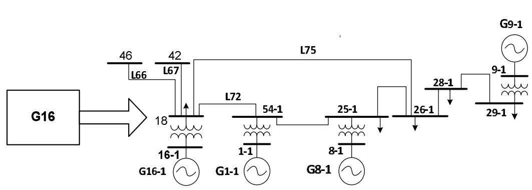

Fig. 2: G16 equivalent with $P_{G16} = P_{G16\text{-}1} + P_{G1\text{-}1} + P_{G8\text{-}1} + P_{G9\text{-}1}$, G16-1 parameters are same as those of G16 while G1-1, G8-1 and G9-1 have the same parameters as G1, G8 and G9 respectively.

Transmission lines are modeled using standard π circuit, and all loads are modeled as constant impedance. Turbine generator rotor is modeled as a six mass mechanical system comprising four stage turbine, i.e., high pressure (HP), intermediate pressure (IP), low pressure A (LPA), low pressure B (LPB) presented in Fig. 3.

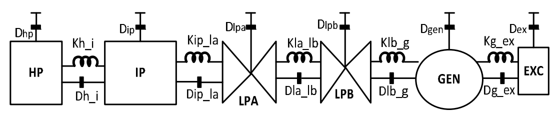

Fig. 3: Six mass rotor model for SSR studies

Mechanical data for turbine generator is taken from I[st] benchmark model for SSR studies [9] and scaled appropriately to match the generator size and total inertia of the unit. In studied test network G1-G8 are originally equipped with slow dc excitation control. The system is stable with uncompensated lines but starts to oscillate with compensated lines. Therefore, dc excitation system of G1, G8 and G9 is replaced with fast acting static excitation system and PSS.

VSC HVDC Modeling

The two terminals VSC based HVDC transmission system mainly consists of two converter stations connected by a dc cable. DIgSILENT PowerFactory provides a PWM (pulse width modulation) converter model that represents a self commutated, voltage sourced AC/DC converter. At the fundamental frequency, the ideal converter can be modeled by a DC voltage controlled AC voltage source conserving active power between AC and DC side.

$$U_{Acr} = K_0 Pm_r U_{DC} \tag{1}$$

$$U_{Acr} = K_0 Pm_r U_{DC} \tag{2}$$

The active power conservation between AC and DC side can be written as

$$P_{Ac} = Re\,(\underline{U}_{AC}\,\underline{I}^{*}_{AC}) = U_{DC}\,I_{DC} = P_{DC} \qquad (3)$$

Where U_{ACr} *and* U_{ACi} are real and imaginary part of *AC*-voltage *(RMS- value),* K_0 is a constant depending on the modulation method, Pm_r and Pm_i are real and imaginary part of modulation index, U_{DC} is *DC* voltage, $\underline{U}_{Ac}$ is *AC* phasor voltage and I_{-AC} is conjugate complex value of *AC* current phasor .

A *dq*- current controller presented in Fig. 4 forms an inner loop control, fastest stage of a PWM converter controller. The input currents to the controller are the converter's AC currents expressed in *dq* reference frame. The reference currents are obtained from the dc voltage controller or power controller as one of the converters controls the dc voltage and the other controls the dc link power. The output signals P_{md} and P_{mq} are defined in the same reference frame as input currents and transformed back to a global reference frame using the same reference angle. The ac bus voltage/dc voltage controller and power (P/Q) controller form an outer loop control.

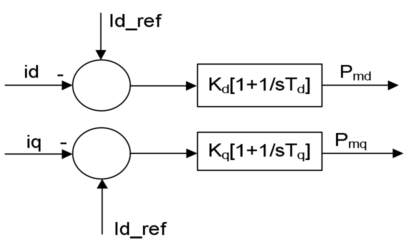

Fig. 4: Block diagram of current controller

Where P_{md} and P_{mq} are pulse width modulation index in *d* and *q* axis.

TCSC Modeling

The TCSC is modeled as a fixed capacitor in parallel with variable inductive reactance (TCR). The TCR and effective TCSC reactance are controlled by firing angle α, and are given by the following equations

$$X_L(\boldsymbol{\alpha}) = X_L \frac{\boldsymbol{\pi}}{\boldsymbol{\pi} - 2\boldsymbol{\alpha} - sin\,2\boldsymbol{\alpha}} \qquad (4)$$

$$\begin{aligned} X_{TCSC}(\boldsymbol{\alpha}) = &-\frac{X_c^2}{(X_c - X_L)}\frac{(2(\boldsymbol{\pi}-\boldsymbol{\alpha}) + sin(2(\boldsymbol{\pi}-\boldsymbol{\alpha})))}{\boldsymbol{\pi}} \\ &+ \frac{4X_c^2}{(X_c - X_L)}\frac{cos^2(\boldsymbol{\pi}-\boldsymbol{\alpha})}{(\boldsymbol{\kappa}^2 - 1)}\frac{[\boldsymbol{\kappa}\tan\boldsymbol{\kappa\beta} - \tan\boldsymbol{\beta}]}{\boldsymbol{\pi}} - X_c \end{aligned} \qquad (5)$$

$$where\ \boldsymbol{\kappa} = \sqrt{\frac{X_c}{X_L}} \qquad (6)$$

For practical TCSC implementations, **κ** is typically between 2 and 4[3, 10]. TCSCs are usually operated such that $\frac{X_{TCSC}}{X_C}$ is between 2 and 3[3, 10].

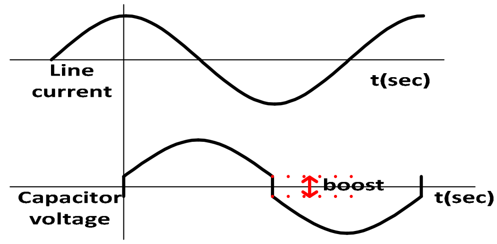

Fig. 5: Illustration of capacitor voltage and line current during TCSC operation

In these studies, TCSC is operated in constant impedance control mode. Thyristors valves are triggered using synchronous voltage reversal approach (SVR) since it provides better damping characteristics in subsynchronous frequency range [11, 12]. Synchronous voltage reversal scheme exploits the fact that capacitor voltage reversal occurs during the thyristor conduction interval. When a thyristor is triggered, a current pulse passes through the thyristor and adds to the line current. Thus, an extra charge is pushed into the capacitor from the thyristor branch. This is, in addition, to the charge due to line current such adding an extra voltage across the capacitor. With no losses, the thyristor valve stops conducting when the capacitor voltage is equal in magnitude but opposite in the direction as it was at the turn –on instant. The maximum reactance boost depends on the actual line current and the duration of the boosting action. Fig. 5 shows the boost in capacitor voltage due to conduction of thyristor valves. Required TCSC impedance can be obtained by an equivalent, instantaneous voltage reversal in the middle of the thyristor conduction interval.

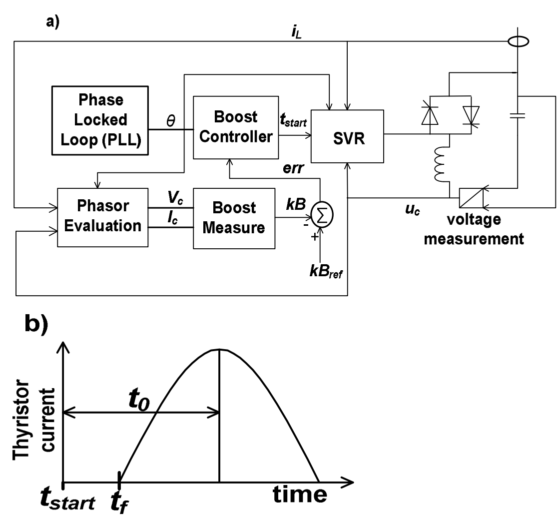

Fig. 6: a) TCSC control structure b) Thyristor Triggering

Fig. 6 illustrates TCSC control structure used in this work. The firing angle is calculated by the impedance control, and start pulse is given to the SVR unit at t_{start} as shown in Fig. 6a, it fires thyristor at t_f. Time t_f is selected such that the thyristor current reaches at its peak with a fixed delay, t_0. The SVR block calculates the firing instant, based on the measured instantaneous values of capacitor voltage and line current [11].

SSR Analysis Method and Results

Series compensation of the lines generates natural electrical frequencies below the synchronous frequency, known as subsynchronous frequencies. Presence of subsynchronous electrical frequencies in the network can cause subsynchronous resonance (SSR). SSR is an electric condition where the electric network exchanges energy with the mechanical system at one or more of the natural frequencies of the combined system. This phenomenon can be divided into two categories[13].

i. Dynamic instability
ii. Transient torques

Dynamic instability is caused when subsynchronous frequency currents interact with the excitation field on the turbine generator rotor to generate torques at the slip frequency (the difference between the synchronous frequency and natural electrical frequency) [14]. The resultant voltages produced by these pulsating torques reinforce the mechanical system oscillations. This interplay between the electrical and mechanical system leads to continuous or sustained growth of mechanical torques resulting into unacceptable shaft stresses.

System electrical disturbances such as capacitor switching, line switching and fault clearing in the network can excite oscillatory torques in generator shaft. The amplitude of these transients torques could be quite high following a disturbance due to SSR phenomenon, though may decay eventually. Each occurrence of high amplitude transient torques removes some of shaft fatigue life. Both, dynamic instability and transient torque amplification are caused by the same interactions.

SSR analysis can be performed using three different techniques, namely frequency scan, eigenvalue analysis and electromagnetic transient simulations [3, 13, 15]. Frequency scan method is based on the calculation of network impedance seen from the study generator. This technique can identify dynamic instability and transient torque amplification due to compensated lines; however, it cannot be applied in networks with VSC HVDC lines. Eigenvalue analysis can indicate potential dynamic instability due to series compensation and VSC HVDC controls, but it is unable to provide information about transient torque amplification. Therefore, electromagnetic transient simulation (EMT) method is used for SSR studies in this paper. The method uses nonlinear models of system components and can detect both, dynamic instability and transient torque amplification problems.

Operation of VSC HVDC in Parallel to Compensated Line

As stated previously, presence of series capacitors in transmission lines produces subsynchronous natural electrical frequencies. Generally, subsynchronous oscillations are damped by the line and transformer resistance. However, the rotating machine will feed energy into the positive sequence subsynchronous currents as the magnetic field setup by these subsynchronous currents rotates at a slower speed than the machines's rotating field. The negative sequence currents act as a brake on the rotor by absorbing the energy to damp the oscillations. Therefore, negative sequence subsynchronous currents induce positive damping and positive sequence subsynchronous currents induce negative damping in the torsional modes[4, 16].

Mechanical damping of the torsional modes is always positive, however, very small. It is due to friction, wind losses and steam flow around the rotor. It is lowest at no load and increases with the load as steam flow increases around the rotor [14, 17].

Series compensation can cause dynamic instability, due to torsional interactions when introduced negative damping is greater than mechanical damping, leading to undamped torques in the shaft of turbine generator. The growth rate of the torques is directly proportional to introduced negative damping.

It is reported in [6, 7] that VSC HVDC controls, in general add positive damping to torsional modes. To investigate the effect of VSC HVDC line operating in parallel to the compensated line, L44 and L71 are compensated by 70%.

$$\text{Compensation level} = \frac{X_c}{X_L} \times 100$$

Where X_c = reactance of the series capacitor
X_L = Inductive reactance of the line

Two VSC HVDC links are installed in the test network. One between bus 54 and bus 53, in parallel to the compensated line L44, second one between bus 50 and bus 18 in parallel to the compensated line L71. Rectifier, sending end is at dc voltage and reactive power control. Inverter, receiving end is at ac voltage and active power control. The power transfer through first and second HVDC link is 100MW and 300MW respectively. Since the aim of the studies is to investigate the influence of

HVDC controls on torsional torques, modeled protection devices are disabled during the studies.

G1 and G16-1 have detailed multi stage steam turbine models attached to them while other generators are modeled using standard generator models with lumped inertia. To perform SSR analysis on G1 using electromagnetic simulation, a three phase fault is introduced at bus 54 at 0.2 sec and cleared after 75ms.

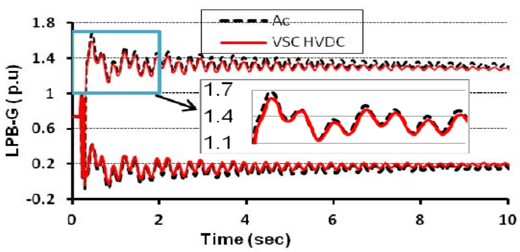

Fig. 7: LPB-G1 mechanical torques; (black shade) with 70% compensated L44 line; (red shade) 70% compensated L44 in parallel with HVDC line.

In Fig. 7 black shade shows mechanical torques in LPB-G shaft section of generator G1when L44 is compensated by 70%, and red shade shows the mechanical torques in the same shaft section of G1 when VSC HVDC line is operating parallel to 70% compensated L44 line. It can be observed that the decay rate of mechanical torques with VSC HVDC is slightly higher than the decay rate of mechanical torques without HVDC line.

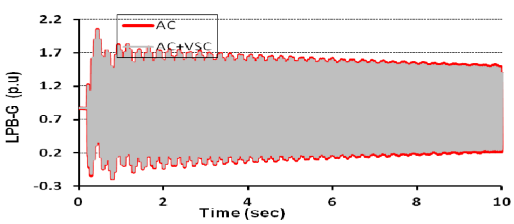

Fig. 8: LPB-G16-1 mechanical torques; (red shade) with 70% compensated L71; (light grey shade) VSC operating parallel to 70% compensated L71.

To perform EMT simulations for G16-1, a three phase fault is introduced at bus 18 at 0.2sec and cleared after 75ms. Fig. 8 presents the torsional torques in LPB-G shaft section of generator G16-1 red curves shows the minimum and maximum values of the mechanical torques without VSC HVDC line and grey shade represents the torques when VSC HVDC is operating parallel to 70% compensated (L71) AC line. Fig. 8 indicates the same influence of VSC HVDC link as is observed in Fig. 7, i.e., a slight improvement in the decay rate of mechanical torques.

Though peak mechanical torques following a brief electrical disturbance are practically independent of the damping level, damping of the modes directly controls the decay rate of oscillations. Same studies are repeated for 50% and 30% compensation levels; results show the same trend in the decay rate of mechanical torques with VSC HVDC line as is observed with 70% compensation level, i.e., very small or a negligible improvement in the decay rate of torsional torques of generator G1 and G16-1.

These studies are also performed for different power transfers through the HVDC link. It is found that amount of power transfer through the HVDC link doesn't affect the decay rate of torsional torques. These results correlate reasonably well with the inherent characteristics of VSC HVDC [7, 18].

Influence of VSC HVDC is also been studied in various contingencies, generated by the outages of the lines (L4, L46, L66, L67 and L72) directly connected to the studied generators G1 and G16-1. Each result has reinforced the previous findings that the decay rate is slightly improved with VSC HVDC.

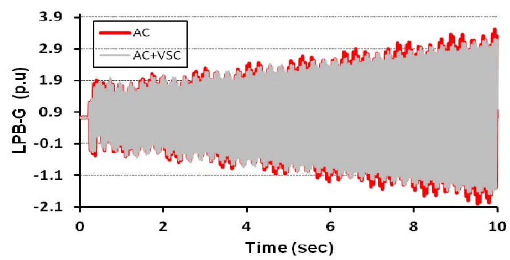

Fig. 9: LPB-G1 mechanical torques in radial configuration; (red shade) with 70% compensated AC line; (light grey shade) VSC operating parallel to 70% compensated AC line.

It is well known that generators operating radially to the compensated are at higher risk of SSR. Simultaneous outage of L46 and L4 connects the generator G1 radially to the compensated line L44. Fig. 9 shows the mechanical torques in LPB-G shaft section of G1 with and without VSC HVDC in N-2 contingency. It can be observed that growth rate is slightly lower with VSC, but it is not able to stabilize the system.

Transient torque amplification due to SSR produces high amplitude mechanical torques and each occurrence results in some loss of shaft fatigue life. Fig. 10 shows the number of torque cycles versus the magnitude of torsional torques to initiate cracks in the shaft[19]. It can be observed that the horizontal axis is divided into two regions, marked as high cycle fatigue region and low cycle fatigue region. In high cycle region, amplitude of the torques is low, and number of cycles to crack initiation is extremely high. In contrast, in low cycle fatigue region, amplitude of the torques is high, therefore, number of torque cycles to initiate crack is small. The black solid line curve is (taken from [19]) a typical life expenditure for a shaft section of turbine generator with base torque value of 0.44 p.u. Red dotted line is obtained by scaling the data with base torque value of 0.74p.u. For red curve, the threshold value of torque at which no further fatigue damage accumulates is 0.95 p.u.

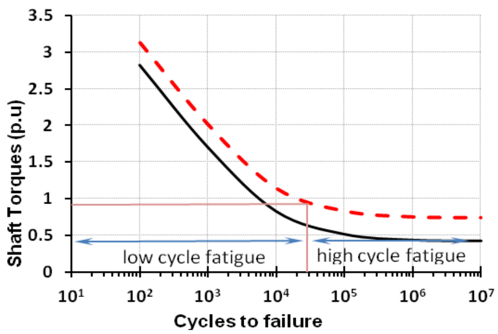

Fig. 10: Typical shaft life expenditure curve

Studies are carried out to assess the influence of VSC HVDC system on transient torque amplification by enabling the modeled protection in the HVDC system.

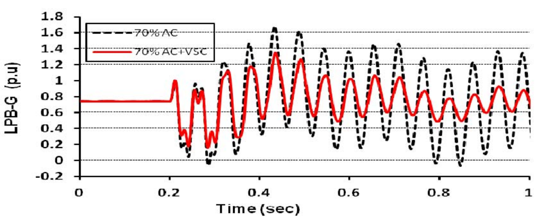

Fig. 11: Transient torque analysis for LPB-G1 shaft section with and without VSC HVDC for 70% compensation

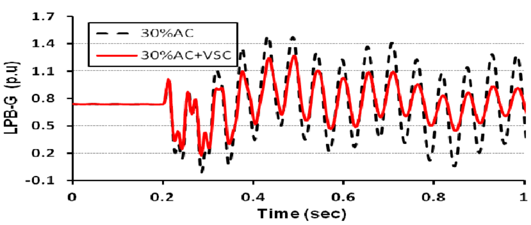

Fig. 12: Transient torque analysis for LPB-G1 shaft section with and without VSC HVDC for 30% compensation

The change in the mechanical torque is directly proportional to induced current in the stator following a disturbance. Presence of HVDC system reduces this induced current and consequently amplitude of torsional torques. Fig. 11 shows clearly that installation of VSC HVDC system has reduced the peak mechanical torque magnitude from 1.67p.u to 1.34 p.u. The amplitude of mechanical oscillations with VSC HVDC, drops below the threshold level after experiencing 9 cycles of low cycle fatigue, within 0.75seconds. Number of cycles experienced before the torques amplitude falls below the (low cycle fatigue) endurance level of shaft decides the accumulated fatigue due to the event. It can be observed from Fig. 7 that with 70% compensation without HVDC system torsional torques amplitude is higher than threshold level (0.95 p.u) even after 10 seconds.

Fig. 12 demonstrates the same positive contribution of VSC HVDC system in parallel with 30% compensated line. The magnitude of the peak torques is reduced from 1.47 p.u to 1.23 p.u, and after only 6 cycles, the amplitude of torques drops below 0.95p.u.

Influence of TCSC on SSR

Thyristor controlled series capacitors provide fast and controllable series compensation of transmission lines. Many studies have been performed to derive accurate dynamic and analytical models [20-23]. Effect of TCSC structure and synchronization response on subsynchronous damping has been investigated in [10]. Impact of TCSC control methodologies on subsynchronous oscillations is explored in [24].

TCSCs exhibit different subsynchronous frequency characteristics from fixed series capacitors, reducing the negative damping of the torsional modes. This paper explores the effect of TCSC on SSR when it is operating in parallel to heavily (fixed series) compensated line in constant impedance control mode. Operation of TCSC in parallel with VSC HVDC line is also studied.

L44 is 70% compensated with fixed series capacitor and L45 is compensated 70% using TCSCs. TCSC parameter are given below

$$\boldsymbol{\kappa} = \sqrt{\frac{X_C}{X_L}} = 2.85,\ C = 64.96\boldsymbol{\mu}F,\ \ L = 19.09mH$$

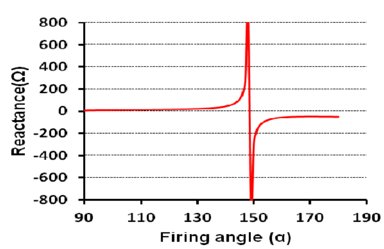

Fig. 13: TCSC steady state impedance characteristics

Fig. 13 reveals the reactance characteristics of the implemented TCSC as a function of firing angle. These characteristics exhibit a parallel resonance frequency at 149°, around this angle small change in the firing angle results in dramatic changes in the TCSC impedance. For 70% compensation, TCSC is operated at 153º.

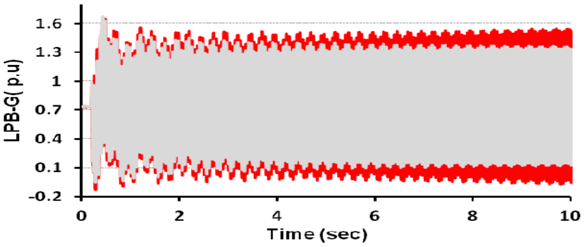

Fig. 14: LPB-G1 mechanical torques; (red) with fixed Series compensation in both lines; (grey shade) L45 70% compensated with fixed capacitor and L44 70% compensated with TCSC.

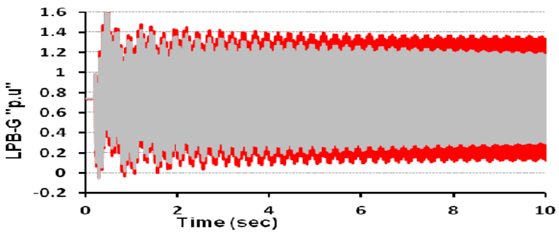

Fig. 15: LPB-G1 mechanical torques; (red) with 70% fixed series compensation in L44 and 70% compensation with TCSC in L45; (grey shade) L44 and L45 compensated by 70% with TCSCs.

It can be observed from Fig. 14 that the system is unstable (red shade) when L44 and L45 are compensated 70% with fixed series capacitors. It becomes stable (grey shade) when one of the parallel lines, L44 is compensated with TCSC and L45 is compensated with fixed capacitors. TCSC impedance control mode is the most basic control; decay rate of mechanical torques can be improved with the addition of SSR damping control. Fig. 15 shows that the decay rate is improved when both lines are compensated 70% with TCSCs.

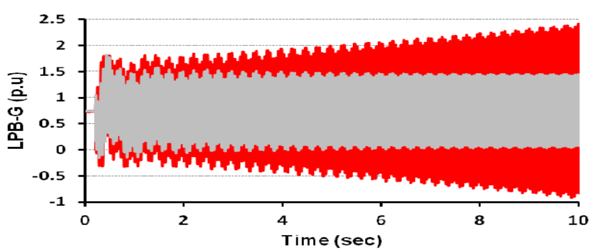

Fig. 16: LPB-G1 mechanical torques in N-1 contingency; (red) with 70% fixed series compensation in L44 and L45; (grey shade) 70% compensation in L44 and L45 with TCSCs.

Fig. 16 demonstrates the effectiveness of TCSCs in improving the system stability in N-1 contingency, generated by the outage of L46. Red shade shows increased growth rate of mechanical torques with 70% fixed series compensated system, and grey shade illustrates mechanical torques with 70% TCSCs compensation in N-1 contingency.

Fig. 17 below shows mechanical torques (red shade) in LPB-G shaft section of G1when L44 is compensated 70% with TCSC and VSC HVDC is operating in parallel. It can be observed that the system is stable, and decay rate of mechanical torques is similar to the instant, when both L44 and L45 are compensated with TCSCs.

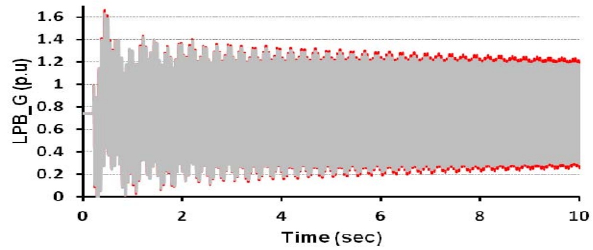

Fig. 17: LPB-G1 mechanical torques;(grey shade) with 70% TCSC compensation in L44 and L45, (red shade) line L44 compensated with TCSC, L45 disabled and VSC HVDC operating in parallel.

Conclusions

SSR analysis in a large meshed AC/DC network shows that in general, VSC HVDC controls adds minor positive damping in torsional modes but are unable to increase the decay rate of torsional torques significantly or stabilize the unstable system. The power transfer through HVDC link does not affect the decay rate of mechanical torques. Results of the performed analysis lead to the conclusion that HVDC controls do not influence "the state of dynamic instability of the compensated system" due to SSR. However, VSC HVDC system reduces the magnitude of peak torques, and number of cycles that inflict low cycles fatigue.

Though, no negative damping of torsional modes due to VSC controls is observed in the studied cases, different control setting and strategies could result into different results.

TSCSs have capabilities to stabilize the system, even with most basic control structure. Decay rate of the mechanical torques can be improved with addition of another control. In the studied system operation of VSC HVDC in parallel to TCSC, compensated line does not affect the decay rate of mechanical torques considerably.

The study's results indicate that the transmission configuration that includes two heavily (fixed series capacitors) compensated parallel lines exposes generators to high risk of SSR; due to dynamic instability and transient torque amplification.

The transient torque amplification problem, due to SSR is significantly reduced when one of the two parallel lines is compensated with series capacitors, and other line is replaced with VSC HVDC. However, dynamic instability problem is not improved or worsened with VSC HVDC operation.

TCSC compensated line operating parallel to series compensated line can mitigate SSR problem effectively.

Transmission configuration that includes VSC HVDC operating in parallel to TCSC compensated line can eliminate the risk of SSR.

References

[1] D. N. Walker, C. E. J. Bowler, R. L. Jackson, and D. A. Hodges, "Results of subsynchronous resonance test at Mohave," *IEEE Transactions on Power Apparatus and Systems,* vol. 94, no. 5, pp. 1878-1889, 1975.

[2] M. Bahrman, E. V. Larsen, R. J. Piwko, and H. S. Patel, "Experience with HVDC - Turbine-Generator Torsional Interaction at Square Butte," *Power Apparatus and Systems, IEEE Transactions on,* vol. PAS-99, no. 3, pp. 966-975, 1980.

[3] K.R.Padiyar, *Analysis of subsynchronous Resonance in Power Systems*. Boston,London: Kluwer Academic Publisher, 1999

[4] L. A. Kilgore, L. C. Elliott, and E. R. Taylor, "The Prediction and Control of Self-Excited Oscillations Due to Series Capacitors in Power Systems," *IEEE Transactions on Power Apparatus and Systems,* vol. PAS-90, no. 3, pp. 1305-1311, 1971.

[5] E.R. Taylor L.A.Kilgore, D.G.Ramey, R.G.Farmer, E.Katz, A.L.Schwalb, "Solutions to the Problems of Subsynchronous Resonance in Power Systems with Series Capacitors," in *Proc.*, 1973, vol. 35, pp. 1129-1136.

[6] N. Prabhu and K. R. Padiyar, "Investigation of Subsynchronous Resonance With VSC-Based HVDC Transmission Systems," *IEEE Transactions on Power Delivery,* vol. 24, no. 1, pp. 433-440, 2009.

[7] J-H. Ying, H. Duchen, K. Linden, M. Hyttinen, P. F. de Toledo, T. Tulkiewicz, A. K. Skytt, and H. Bjorklund, "Improvement of subsynchronous torsional damping using VSC HVDC," in *Proc. International Conference on Power System Technology, 2002.* , 2002, vol. 2, pp. 998-1003 vol.2.

[8] P.Pal and B.Chauduri, *Robust Control in Power Systems*. New York: Springer Science & Business Media, 2005

[9] IEEE Subsynchronous Resonance Task Force, "First benchmark model for computer simulation of subsynchronous resonance," *IEEE Transactions on Power Apparatus and Systems,* vol. 96, no. 5, pp. 1565-1572, 1977.

[10] M. H. Abardeh and J. Sadeh, "Effects of TCSC parameters and control structure on damping of sub-synchronous resonance," in *Proc. 4th International Power Engineering and Optimization Conference (PEOCO), 2010* 2010, pp. 26-32.

[11] L. Angquist, G. Ingestrom, and H-Ake. Jonsson, "Dynamical Performance of TCSC Schemes," CIGRE' 1996:14-302

[12] L. Qianjin, Z. Changchun, L. Angquist, and C. Rehtanz, "A novel active damping control of TCSC for SSR suppression in a radial corridor," presented at the 2008 Third International Conference on Electric Utility Deregulation and Restructuring and Power Technologies, 2008. DRPT 2008.

[13] P.M.Anderson, B.L.Agrawal, and J.E.Van Ness, *Subsynchronous Resonance in Power Systems*. New York: IEEE Press, 1990

[14] C. E. J. Bowler, D. H. Baker, N. A. Mincer, and P. R. Vandiveer, "Operation and Test of the Navajo SSR Protective Equipment," *IEEE Transactions on Power Apparatus and Systems,* vol. PAS-97, no. 4, pp. 1030-1035, 1978.

[15] IEEE Committee Report, "Reader's guide to subsynchronous resonance," *Power Systems, IEEE Transactions on,* vol. 7, no. 1, pp. 150-157, 1992.

[16] J. W. Ballance and S. Goldberg, "Subsynchronous Resonance in Series Compensated Transmission Lines," *IEEE Transactions on Power Apparatus and Systems,* vol. PAS-92, no. 5, pp. 1649-1658, 1973.

[17] D. H. Baker, G. E. Boukarim, R. D'Aquila, and R. J. Piwko, "Subsynchronous resonance studies and mitigation methods for series capacitor applications," in *Proc. IEEE Power Engineering Society Inaugural Conference and Exposition in Africa, 2005* 2005, pp. 386-392.

[18] J.Arrillaga, Y.H.Liu, and N.R.Watson, *Flexible Power Transmission: The HVDC Options*. Chichester: Jhon Wiley & Sons, 2007

[19] D. N. Walker, S. L. Adams, and R. J. Placek, "Torsional Vibration and Fatigue of Turbine-Generator shafts," *Power Apparatus and Systems, IEEE Transactions on,* vol. PAS-100, no. 11, pp. 4373-4380, 1981.

[20] C. R. Fuerte-Esquivel, E. Acha, and H. Ambriz-Perez, "A thyristor controlled series compensator model for the power flow solution of practical power networks," *IEEE Transactions on Power Systems,* vol. 15, no. 1, pp. 58-64, 2000.

[21] S. G. Jalali, R. H. Lasseter, and I. Dobson, "Dynamic response of a thyristor controlled switched capacitor," *IEEE Transactions on Power Delivery,* vol. 9, no. 3, pp. 1609-1615, 1994.

[22] P. Mattavelli, G. C. Verghese, and A. Stankovic, "Phasor dynamics of thyristor-controlled series capacitor systems," *IEEE Transactions on Power Systems,* vol. 12, no. 3, pp. 1259-1267, 1997.

[23] D. Jovcic and G. N. Pillai, "Analytical modeling of TCSC dynamics," *IEEE Transactions on Power Delivery,* vol. 20, no. 2, pp. 1097-1104, 2005.

[24] L. A. S. Pilotto, A. Bianco, W. F. Long, and A. Edris, "Impact of TCSC control methodologies on subsynchronous oscillations," *IEEE Transactions on Power Delivery,* vol. 18, no. 1, pp. 243-252, 2003.